Geophysical Research Letters

RESEARCH LETTER
10.1029/2020GL089062

Special Section:
Understanding carbon-climate feedbacks

Key Points:

- After controlling for stress-loading, mechanical weathering rates—measured in situ—still strongly correlate with moisture and temperature
- Vapor pressure's influence on crack-tip subcritical cracking processes appears to govern observed trends, independent of stress magnitude
- Recognizing this novel facet of weathering's climate-dependence will enhance understanding of all climate-dependent systems like the carbon cycle and landscape evolution

Supporting Information:

- Supporting Information S1

Correspondence to:
M. C. Eppes,
meppes@uncc.edu

Citation:
Eppes, M. C., Magi, B., Scheff, J., Warren, K., Ching, S., & Feng, T. (2020). Warmer, wetter climates accelerate mechanical weathering in field data, independent of stress-loading. *Geophysical Research Letters*, *47*, 2020GL089062. https://doi.org/10.1029/2020GL089062

Received 2 JUN 2020
Accepted 30 OCT 2020

Warmer, Wetter Climates Accelerate Mechanical Weathering in Field Data, Independent of Stress-Loading

M. C. Eppes[1], B. Magi[1], J. Scheff[1], K. Warren[2], S. Ching[1], and T. Feng[3]

[1]Department of Geography & Earth Sciences, University of North Carolina at Charlotte, Charlotte, NC, USA,
[2]Department of Civil and Environmental Engineering, University of North Carolina at Charlotte, Charlotte, NC, USA,
[3]Department of Computer Science, University of North Carolina at Charlotte, Charlotte, NC, USA

Abstract Weathering is a foundational process in most Earth systems, but there has been a lack of data directly quantifying what influences *mechanical* weathering. Here we use multiple years of *in situ* field data, "listening" to acoustic emissions of naturally cracking rocks, to test a hypothesized link between climate and subcritical crack-tip processes (i.e., the bond-breaking mechanism thought to embody most mechanical weathering). Our results challenge the assumption of a singular dependence of mechanical weathering on stresses. We find that mechanical weathering rates exponentially increase as functions of atmospheric vapor pressure (VP), temperature, and relative humidity, even when controlling for stress-loading. VP exerts the most pronounced influence on the observed mechanical weathering rates. Put in the context of global climate change, our results underscore the potential for climate-dependent subcritical crack-tip processes to influence all weathering-allied problems including the long-term stabilization of the climate by weathering-carbon-cycle feedbacks.

Plain Language Summary Weathering refers to the mechanisms by which rocks physically and chemically break down into soil, sediment, and dissolved molecules. Chemical weathering rates are frequently inferred to be strongly coupled to climate, because chemical reactions depend on factors like moisture and temperature. In past studies, climate has been connected to physical weathering only through its influence on stress-inducing processes like freezing or temperature cycling. In this study, we use field observations of the sounds that natural rock cracking makes and find that cracking accelerates in warmer, wetter conditions, even when controlling for stresses. Thus, this study provides field data to support a climatic influence on weathering via a pathway—molecular bond-breaking at crack-tips—that is additional to, and distinct from, how climate may influence stresses or chemical weathering. Accordingly, any system connected to weathering, such as Earth's carbon cycle, surface erosion, or biosphere, could be impacted by this additional process of accelerated rock breakdown during warmer and wetter climates, such as those predicted under modern global warming trends.

1. Introduction

Accurate characterizations of how climate controls weathering, the in situ breakdown of rock, are essential because weathering drives erosion and soil formation (Murphy et al., 2016; Richter et al., 2019), impacts biomes (Lu & Hedin, 2019) including the evolution of human life (Kasting, 2019), degrades civil infrastructure (Phillipson et al., 2016), and—crucially—influences the rate of atmospheric CO_2 uptake by the lithosphere, which stabilizes climate on geological time scales (e.g., Isson et al., 2020; Macdonald et al., 2019; Walker et al., 1981).

Currently, however, published quantifications of global-climate-weathering connections (e.g., Rugenstein et al., 2019; Winnick & Maher, 2018) do not take into consideration climate's influence on the *mechanical* component of rock weathering, the lengthening of fractures caused by stresses at Earth's surface—hereafter referred to as "cracking." Yet chemical weathering—and most other surface processes—are limited without the breakdown and porosity facilitated by cracking (e.g., Ferrier & West, 2017; Holbrook et al., 2019). Prior work clearly links mechanical weathering to climate (e.g., Collins et al., 2018; Draebing et al., 2017; Enzel et al., 2012; Girard et al., 2013; Marshall et al., 2017; Pederson et al., 2000; Viles, 2005) but also shows that the climate-cracking system is complex (e.g., Viles, 2013). We therefore lack quantitative data to support many common assumptions regarding the factors that govern natural mechanical weathering variability (Scott & Wohl, 2019; Sklar et al., 2017).

Traditionally, climate-mechanical weathering studies have centered on identifying the environmental conditions that maximize stresses associated with individual stress-loading processes like freezing, thermal cycling, or mineral hydration (e.g., Fletcher et al., 2006; Hall & André, 2001; Hallet et al., 1991; Matsuoka, 1990; Rempel et al., 2016). A new fracture mechanics conceptual framework for understanding mechanical weathering, however, advocates that climate plays an additional role in natural rock cracking via subcritical crack-tip bond-breaking (Eppes & Keanini, 2017; background). Eppes and Keanini (2017) support this hypothesis with a review of published experimental data and with a physical model demonstrating that under constant stress-loading, linear increases in moisture can result in exponential increases in cracking rates. To our knowledge, however, no study has documented such an effect in a natural setting. To do so requires a study design that can simultaneously monitor natural cracking and environmental factors like temperature and moisture, while also isolating how those factors relate to rock cracking, independent of how they influence rock stresses. The data set must also be relatively long (months to years) as natural cracking is predominately slow and nonlinear (e.g., Collins et al., 2018).

In this study, we seek to document whether a stress-independent climate-dependence of mechanical weathering can be observed in natural settings. To control for stress, we focus on boulders rather than outcrops so that the complicating influences of gravitational or tectonic stresses are minimized. Following methods of Warren et al. (2013), we continuously measure in situ rock cracking for ~4 total years using acoustic emission (AE) sensors attached to two natural boulders. Importantly, for both datasets the stress-triggers for cracking have already been characterized (Ching, 2018; Eppes et al., 2016), allowing us to confidently control for stresses and to document any remaining influence of moisture and temperature on cracking. Finally, in order to determine how our results may translate over larger time and space scales—under realistic climatic conditions—we explore the data in the context of simulated CO_2-driven global warming.

The data presented are consistent with a key additional pathway—subcritical crack-tip processes—by which climate may modulate weathering rates, even over long time scales. This result strongly diverges from the long-held, implicit assumption of most mechanical weathering research on Earth and other planets that rock fracturing rates hinge solely on stresses.

2. Background

Rock cracking brought on by tectonic, topographic, and environmental stresses arising at Earth's surface (~0–500 m depth; e.g., Moon et al., 2020) embodies mechanical weathering. Because the vast majority of such stresses are less than rock's critical strength, mechanical weathering is likely governed by subcritical cracking (Eppes & Keanini, 2017; Eppes et al., 2018; Hall, 1999; Martel, 2011; Molnar, 2004; Stock et al., 2012; Walder & Hallet, 1985). "Subcritical cracking" is the generic term for any slow, steady crack growth proceeding under cyclic or static stresses lower than the material's critical strength (where critical strength is quantified by material properties like tensile strength or fracture toughness). Subcritical cracking is also known as time-dependent cracking, brittle creep, progressive failure, and environmental cracking (see fracture mechanics textbooks like Anderson, 2005).

Explicitly acknowledging that mechanical weathering proceeds subcritically is significant because the molecular bond-breaking processes of subcritical cracking innately and dominantly occur through chemo-physical processes like stress corrosion (e.g., Brantut et al., 2013). In turn, these subcritical bond-breaking processes—including fatigue—are all driven by stress-enabled chemical reactions involving rock molecules and crack-tip pore-water, the latter of which may be in either liquid or gaseous phases (e.g., Atkinson, 1987). Because chemical reactions are part and parcel to all subcritical cracking, subcritical cracking rates are not only predicated on stress magnitude, but *also* on all of the factors upon which chemical reaction rates are dependent like moisture and temperature (e.g., Chen et al., 2019), similar to the climate-dependence of chemical weathering reaction kinetics (e.g., Hilley et al., 2010). Eppes and Keanini (2017) hypothesize that this stress-independent climate-dependence of subcritical cracking is applicable to all mechanical weathering on Earth. Here we seek to test this hypothesis for the first time in a natural setting, where stress and cracking processes are necessarily more complex.

3. Methods

3.1. Field Deployment

Two ~25 cm diameter rounded boulders were collected from an unvegetated boulder bar in the Santa Ana wash, California, comprising identical rock types: 1–5 mm average grain size, and nonfoliated hornblende-biotite granodiorites. Thus, these boulders share a similar recent exposure history, having both been periodically tumbled up until their collection, removing, we assume, any preexisting *major* cracks through impact abrasion. We also assume, however, that smaller interior imperfections differ between the rocks due to differences in long-term exposure and/or grain-scale heterogeneity.

The boulders were positioned in open sun (Figure S1) in a humid temperate deciduous forested area (North Carolina [NC]: 35.2986°N, −81.0880°W, 235 masl) and a semiarid temperate shrubland (New Mexico [NM]: 34.3379°N, −106.7414°W, 1603 masl) from June 2010 to May 2011 and from August 2011 to July 2014 respectively. Not including days marked by power or other equipment malfunction, we collected a total of about 7,000 h of data in NC and 26,000 h in NM.

3.2. AE Data

The boulders were identically equipped with six 100–450 kHz AE sensors with an internal preamp gain of 40 dB (Physical Acoustics Corporation, PKI51). AE sensors were programmed to monitor cracking whose energy exceeded our user-defined threshold of 45 dB. Rather than report on "hits" from individual AE sensors, here we only consider larger AE "events"—emissions registered simultaneously by four or more AE sensors. We present AE data as numbers of events, a proxy for the magnitude of cracking (Grosse & Ohtsu, 2008). All sensors were calibrated (Warren et al., 2013), and the possible effects of background noise on AE monitoring were closely scrutinized (Data Supplement in Eppes et al., 2016).

3.3. Meteorological Data

Atmospheric temperature (T), relative humidity (RH), and precipitation were measured adjacent to the boulders (~2.5 m distance) at 1-min resolution using a Campbell Scientific weather station. Because we seek to examine the role of atmospheric conditions in driving cracking, we do not consider the conditions on the rock surface or in its interior. Instead, we assume that atmospheric conditions proportionally transfer to the rock at time scales on the order of an hour (below), a necessary assumption for interpreting results as reflecting crack-tip subcritical processes. Data during the monitoring periods were comparable with records of nearby weather stations (Figure S2).

Vapor pressure (VP), which reflects the air's total water vapor content, was calculated from measured T and RH using:

$$\mathrm{VP} = \frac{\mathrm{RH}}{100} \times \mathrm{VP_{sat}}$$

$$\mathrm{VP_{sat}} = 6.11\,\mathrm{hPa} \times \exp\left[\frac{L_v}{R_v}\left(\frac{1}{273\,K} - \frac{1}{T}\right)\right]$$

where $\mathrm{VP_{sat}}$ is the saturation VP analytically determined from the Clausius-Clapeyron equation using T in degrees Kelvin, $L_v = 2.5 \times 10^6$ J kg^{-1} is the latent heat of vaporization, and $R_v = 461$ J kg^{-1} K^{-1} is the gas constant for water vapor (e.g., Chapter 6 of Tsonis, 2002).

3.4. Controlling for Stress

In general, subcritical cracking rates are strongly predicated on the magnitude of external stress-loading experienced by the cracking solid, regardless of the source(s) of that stress. Prior work on the datasets by Eppes et al. (2016) and Ching (2018) identified two primary sources of stresses causing cracking in the two

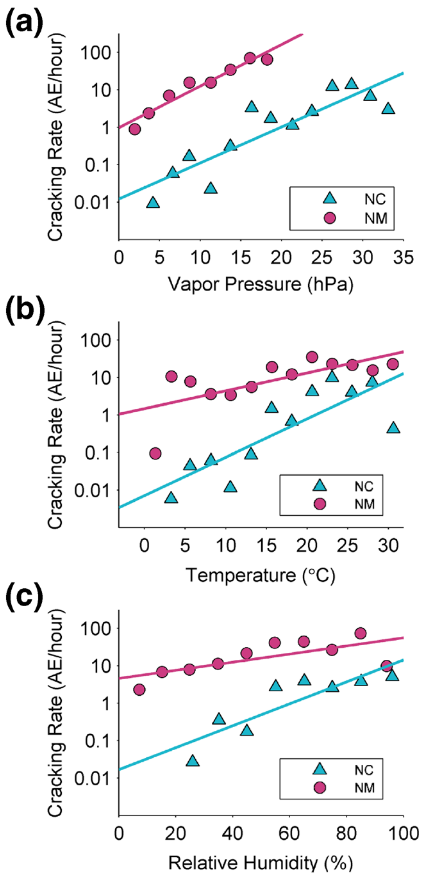

Figure 1. Hourly mean cracking rates within "bins" of T, RH, and VP. Calculated (Table S1) for the NM and NC boulders as a function of ambient (a) VP (bin width 2.5 hPa), (b) T (bin width 2.5°C), and (c) RH (bin width 10%). NC, North Carolina; NM, New Mexico; RH, relative humidity; T, temperature; VP, vapor pressure.

datasets: (1) freezing and (2) thermal cycling brought on by both weather and daily insolation.We thus assume these boulders, sitting stationary on the ground, experienced no other signficant sources of stress, allowing us to control for both stress source and magnitude.

To isolate the source of stresses analyzed in our study, we exclude days containing any minutes with subfreezing temperatures ($T \leq 0$°C). This filter is based on the conservative assumption that frozen water is unlikely to remain in boulder interiors more than 24 h after experiencing freezing temperatures.

Assuming that all remaining nonfreezing-related cracking in the datasets is driven by thermal stresses, we employ parameters, based on T, as proxies for the magnitude of those stresses. Published numerical modeling identifies three primary T-based parameters that can scale with thermal stress magnitude in rock: (1) absolute temperature (T), (2) rate of temperature change (dT/dt), and (3) diurnal temperature range (Daoud et al., 2020; Molaro & Byrne, 2015; Ravaji et al., 2019). Our analysis suggests no statistically significant relationship between diurnal temperature range and cracking rate (Figure S3), so we concentrate on T and dT/dt as the thermal stress proxies. As would be expected, our data show strong positive correlations at both field sites between cracking rates and both T and dT/dt (Figure 1 and Figure S3; Table S1), supporting our assumption that they represent the key stress-drivers controlling cracking rate. We acknowledge here—and discuss later—the complexity that arises in the study design whereby T may act as a source of stress, but also as a factor that may impact crack-tip processes.

Finally, to control for stress *magnitude*, we studied cracking rates segregated into periods of time when the rocks experienced limited ranges (bins) of the thermal stress proxies T or dT/dt (e.g., ±2°C or ±0.1°C/min), and we examined how those cracking rates—under each distinct stress magnitude—related to T, RH, and VP. We reason that if climate influences cracking independent of stresses, we should observe correlations between measured cracking and T, RH, and/or VP for each level of stress magnitude given as a small range of T or dT/dt.

3.5. Data Processing and Analysis

We chose an hourly analysis for the data because rock conditions can lag atmospheric conditions (e.g., Matsukura & Takahashi, 2000). To make this decision, we estimated both the time required for thermal signals to penetrate the rock to the depths at which cracking occurred, and the time for ambient vapor to diffuse into the cracks. The majority of measured AE in both rocks was located within 0–10 cm depth (Ching, 2018; Eppes et al., 2016). A measurement of thermal diffusivity from a boulder of identical rock type (1.208 mm^2/s) yields a thermal penetration depth of 4.7 cm per hour. A measured porosity of the upper 5 cm of the same boulder (3.0%–3.7%) implies vapor diffuses to observed cracking depths on time scales of an hour as well (Peng et al., 2012).

We processed all data into hourly averages of T, VP and RH, and hourly totals of AE events (Supplemental Data). Hourly dT/dt was calculated as the maximum per-minute T change recorded in each hour (dT/dt Max). We then organized the data into discrete intervals (bins) of T, RH, VP, and dT/dt Max and calculated cracking rates under the conditions of each bin or in combinations of bins. Using this binning method—as opposed to the prior evaluation of simple, bivariate correlations (Eppes et al., 2016)—accounts for uneven sampling of different ranges of T, VP, RH, and dT/dt Max conditions, permits scrutiny of the relative influence of covarying factors, and allows for isolation of stress magnitudes.

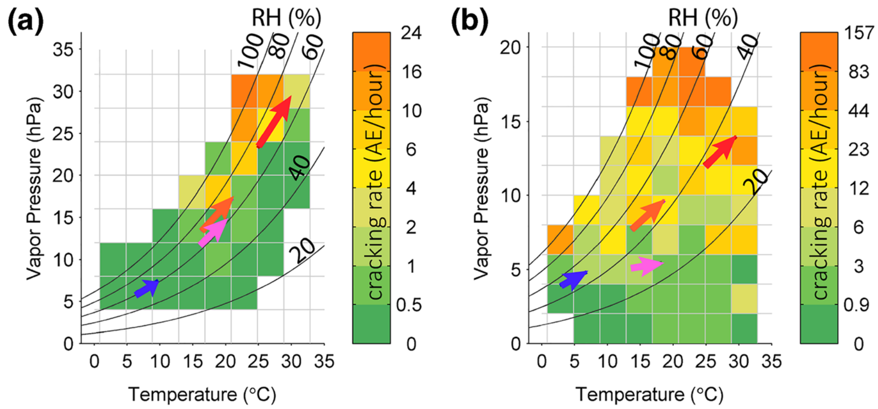

Figure 2. Hourly mean rock cracking rates calculated for coinciding measured hourly average ambient VP (bins of 4 hPa NC; 2 hPa NM) and temperature (bins of 4°C) for (a) NC and (b) NM. Lines of constant RH are overlaid. Modeled changes in seasonal-mean *T*, RH, and VP conditions with RCP8.5 global warming are indicated from the base to the point of the arrows (blue = DJF; pink = MAM; red = JJA; orange = SON). Regression statistics for CR versus VP or *T* within each row or column are in Table S3. NC, North Carolina; NM, New Mexico; RH, relative humidity; *T*, temperature; VP, vapor pressure.

Cracking rates (CR, in AE events/h) in any given bin *i* (CR_i) of Figure 1 are calculated as

$$CR_i = \frac{\sum E_i}{\sum t_i}$$

where $\sum E_i$ is the number of events in bin *i*, $\sum t_i$ is the total number of hours in bin *i*, and bin *i* is defined as a discrete range of either VP, *T*, or RH.

Because of the interdependence of VP, *T*, RH, and the thermal stress proxies, we also calculated CR for paired *T*, RH, VP or d*T*/d*t* conditions ($CR_{i,j}$) to explore CR dependence on the variables under controlled conditions as

$$CR_{i,j} = \frac{\sum E_{i,j}}{\sum t_{i,j}}$$

where $\sum E_{i,j}$ is the number of events in bin (i, j), $\sum t_{i,j}$ is the total number of hours in bin (i, j), and bin (i, j) is defined as a discrete range of combinations of two of the variables *T*, RH, VP, or d*T*/d*t* Max (Figures 2 and 3). Lines of equal RH are indicated in Figure 2 with VP and *T*.

The distributions of cracking rates are strongly positively skewed resulting in large standard deviations (Figures S4 and S5), but our goal—so that results are applicable for climate-related research—is insight built from what multiyear data reveals about the behavior of *mean* cracking rates as a function of VP, *T*, RH, and d*T*/d*t* Max.

Bin ranges in Figures 1–3 and Figures S3–S9 were determined using an iterative approach that maximized (1) the amount of data available for a meaningful calculation in each bin (i.e., reasonable statistics) and (2) the resolution that bin width could provide. We excluded bins with less than 24 h of data as not large enough to be representative. We evaluated a range of bin widths and saw no evidence of artifacts in the results that arose purely from our choices, other than Figure S3B where the smaller data set for NC produces insignificant correlations if smaller bin-sizes are employed.

3.6. Projections of Global *T*, VP, and RH Change

Because global warming tends to reduce RH on land even as it increases *T* and VP (e.g., Byrne & O'Gorman, 2016), we also explore our data in the context of how mechanical weathering rates might be impacted

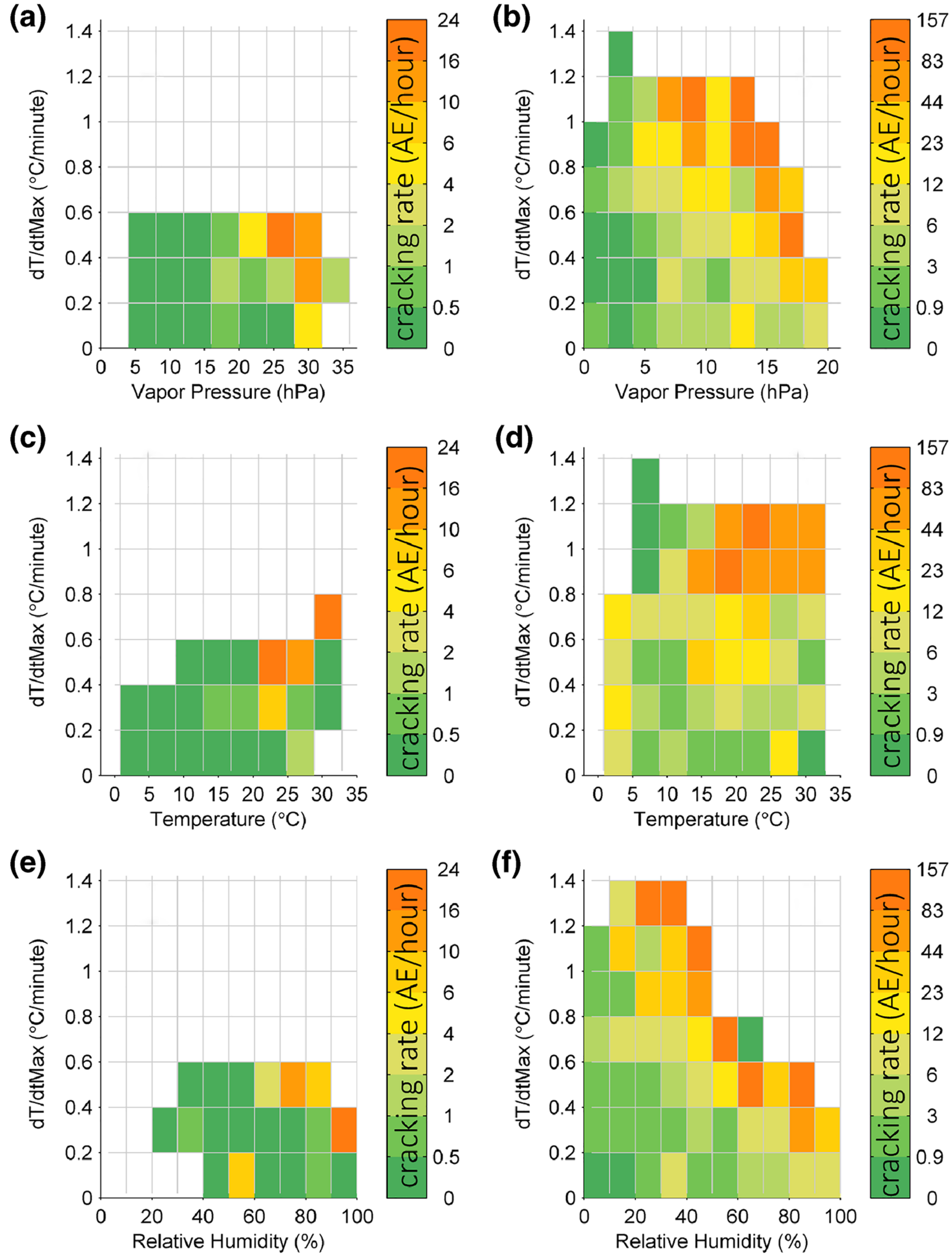

Figure 3. Hourly mean rock cracking rates calculated as a function of coinciding measured hourly maximum per-minute dT/dt (dT/dt Max; bins of 0.2°C/min) versus ambient (a and b) VP (bins of 4 hPa NC; 2 hPa NM), (c and d) temperature (bins of 4°C), and (e and f) RH (bins of 10%) for the boulder in NC (left) and NM (right). Regression statistics for each row and column are in Table S4. NC, North Carolina; NM, New Mexico; RH, relative humidity; VP, vapor pressure.

as a function of realistic covariation of these three variables. For each of 34 climate models in the Coupled Model Intercomparison Project phase 5 (CMIP5; K. E. Taylor et al., 2012), we computed annual-mean and seasonal-mean near-surface climatological fields of T, VP (using specific humidity and air pressure), and RH (using T and VP) for the 1975–2004 period of the historical experiment and for the 2070–2099 period of the "RCP8.5" high emissions experiment. For each model, we differenced the warm-future and historical climatologies to obtain change projections, linearly remapped those projections to a common 1-degree grid, and took multimodel statistics (Figure 4).

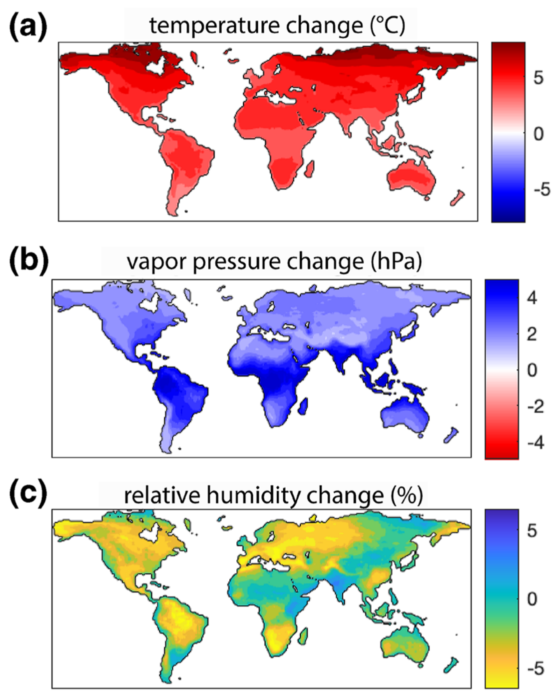

Figure 4. Median projected 21st century changes in (a) temperature, (b) VP, and (c) RH from 34 CMIP5 climate models (RCP8.5 scenario). RH, relative humidity; VP, vapor pressure.

The climate-change trajectories for the two field sites (arrows in Figure 2; Table S2) in *T*-VP-RH space begin at the observed seasonal-mean conditions, and then add the multimodel-median seasonal-mean change projections for *T* and RH at the 1-degree gridpoint nearest each site to obtain the "warmed" seasonal *T* and RH (and thus VP) at each site.

4. Results and Discussion

4.1. Influence of VP, RH, and Temperature on Cracking

We find statistically significant exponential relationships for both study sites between rock cracking rate (CR, in AE events/hour) and VP, *T*, and RH (p-values < 0.05; Figure 1; Table S1). On average, cracking rate doubles for every 2.9 hPa increase in VP, every 4.6°C increase in *T*, and every 19% increase in RH. These relationships between cracking and *T*, RH, VP are obscured if uneven sampling of conditions is not accounted for, and thus had not been identified in past analyses (Ching, 2018; Eppes et al., 2016).

However, since VP, *T*, and RH are all interdependent, relationships in Figure 1 may be misleading. To more carefully characterize each influence, we examine cracking in the context of the VP-*T*-RH system as a whole (Figure 2). If *T* is necessary and sufficient in controlling cracking rates, then cracking should generally increase toward the right on Figures 2a and 2b, but instead the behavior is inconsistent. Similarly, cracking does not consistently increase toward the upper-left as a function of RH. The strongest, and most consistent, relationship is that cracking increases with higher VP, that is, toward the *top* of Figures 2a and 2b. Thus, the influences of *T* and RH on cracking rate (Figure 1) appear to reflect a dependence of CR on VP. Correlations between log(CR) and *T* along each row of Figure 2, and between log(CR) and VP along each column, are given in Table S3; correlations between log(CR) and VP are both stronger and more often significant ($p < 0.05$), confirming the visual impression.

4.2. Stress-Independent Climate Influence on Cracking

Acknowledging that our stress-proxies *T* and d*T*/d*t* Max influence cracking rates (rows in Figure 2; columns in Figure 3), we examine remaining relationships between CR and *T*, VP and RH under the quasi-uniform stress magnitudes represented by each stress-proxy bin. Cracking rates strongly scale with VP for all levels of inferred stress-loading (e.g., within any one column in Figure 2 or row in Figure 3). The influence of RH is similar to VP (Figures 3e and 3f). Regression statistics for CR versus *T*, VP, or RH within each stress-loading bin support these interpretations (Tables S3 and S4).

Further analyses suggest that observed relationships are not an artifact of wetter weather driving temperature changes and thus thermal stress. Past work had identified that the majority of cracking in the two datasets occurred due to abrupt temperature changes brought on by weather (rain or wind) that rapidly cooled the rock surface during periods (midday and sunset) of high antecedent thermal stresses brought on by diurnal insolation (Eppes et al., 2016). When we filter the data to remove times of rainfall onset, however, the relationships between cracking rate and VP and RH are still clear (though somewhat weaker) (Figures S6 and S7; Tables S3 and S4).

Under constant d*T*/d*t*-driven stresses, however—with and without rainfall-onset—cracking does not consistently correlate with *T* (Figures 3c and 3d and Figures S7C and S7D). This could be due to complex location- and time-dependent factors impacting d*T*/d*t* (wind, rain, seasons). In other words, periods of high d*T*/d*t* occurring under overall low *T*—relatively common in the datasets (Ching, 2018; Eppes et al., 2016)—may result in a conflicting influence of *T* on crack-tip processes (slower cracking) versus its influence on stress-loading (faster cracking), thus obscuring correlations between CR and *T* overall. In bedrock or locations with different sources of stresses, a stress-independent relationship between CR and *T* may be clearer.

We interpret the observed stress-independent influence of VP—and to a lesser extent RH and *T*—on cracking as a reflection of the subcritical nature of natural rock fracture, whereby rates of crack-tip bond breaking are influenced by the "environment" of the crack-tip. This interpretation is supported by published experimental and modeling studies—conducted on a full range of rock types—that hold stress constant and measure or calculate subcritical cracking rates under varying temperature and moisture (e.g., Atkinson & Meredith, 1981; Dove, 1995; Eppes & Keanini, 2017; Heap et al., 2009; Nara et al., 2010; Nara et al., 2017; Voigtländer et al., 2018). All of these studies measure exponentially positive moisture- and temperature-cracking relationships similar to those presented herein (Brantut et al., 2013).

Cracking (total observed AE) for the NM boulder is nearly triple that of the NC boulder for a given year, but measured AE energy from each event (Dash, 2015) shows that NC events are characterized by more than double the energy of the NM events. Importantly, because subcritical cracking rates are highly sensitive to how crack length and density impact the stress magnitude "felt" at crack-tips (conceptualized by stress intensity), actual crack-tip stresses cannot be readily controlled for in rocks of this relatively large size (e.g., Lobo-Guerrero & Vallejo, 2006). Thus, prudence is needed when comparing cracking rates for a given set of conditions between two rocks whose interior microcrack characteristics undoubtedly vary and whose experienced covarying *T*, RH, VP, and d*T*/d*t* differ. Nevertheless, we cautiously propose that NM may have more total events due to the higher overall d*T*/d*t*-related stress-loading (double that of NC; Figure S3), while the energy of NC events may be higher due to higher overall VP impacting subcritical crack-tip processes (Figure 1).

4.3. Implications for Long-Term Weathering in Changing Climates

Examining model simulations of *T*, VP, and RH under greenhouse warming, we find that, for any given stress, a warmer Earth should ultimately result in faster mechanical weathering via the hypothesized climate-crack-tip mechanism. Increases in global temperature increase VP nearly everywhere on Earth, due to the ~6% per degree Celsius increase in VP_{sat} with warming (Chadwick et al., 2016). For example, surface warming of about 3°C–5°C (Figure 4a) leads to a median modeled increase in VP of about 2–5 hPa (Figure 4b). In our data set, this VP increase causes a 1.6–3.6 fold acceleration in cracking (Figure 1; Table S1). In contrast, RH is modeled to slightly decrease on land as the climate warms (Figure 4c) (Byrne & O'Gorman, 2016), but increases in cracking rates due to increases in VP appear to outweigh any decreases in cracking rates due to decreases in RH (arrow trajectories in Figure 2). Past warm climates likely experienced even smaller RH decreases with warming (Burls & Fedorov, 2017) and past cold climates apparently *gained* RH as they warmed (Scheff et al., 2017), so our results likely apply to past climate changes as well.

4.4. Limitations and Other Considerations

This study is for a single rock type in two climates, but experimental data (e.g., Brantut, 2013: Gangloff & Harlow, 2017) suggest our results will be applicable for all rock types and climates—noting that extreme cold subcritical cracking studies are rare for rock. We could find no rock subcritical cracking experimental studies that hold VP constant and examine *T* effects lower than ~75C (Meredith & Atkinson, 1985), but *T* clearly impacts subcritical cracking independent of moisture and stress in other materials (Gangloff & Harlow, 2017). Similarly, although we only consider thermal stresses in boulders, physical models and experiments suggest the results should stand for bedrock and also regardless of the types of stresses being experienced (Eppes & Keanini, 2017).

We acknowledge that a broad range of variables, and other stresses besides thermal, alongside a changing climate, will impact the precise climate-mechanical weathering relationships in any given location on Earth. For example, experimental and modeling studies demonstrate that the precise relationships between cracking rate and VP, *T*, and RH will vary in magnitude depending on rock-material properties, crack properties (crack length and density), water chemistry, weathering history, and stress (reviewed in Eppes & Keanini, 2017). Also, in natural settings, VP, *T*, and RH influence the magnitude and type of other stresses not considered herein like ice segregation (e.g., Draebing & Krautblatter, 2019; Murton et al., 2006). Thus, warmer climates may result in lower stresses related to freezing, but the effect of increased VP on cracking rates via crack-tip processes could offset or exceed the effect of decreases in freezing-related stress regimes. Such conflicting roles of temperature and moisture in mechanical weathering will need to be considered in future work.

5. Conclusions

Our field data support the hypotheses (Eppes & Keanini, 2017) that natural mechanical weathering is subcritical in nature and that the majority of Earth's surface and near-surface rocks mechanically weather at rates dependent on factors that impact both stresses and subcritical crack-tip processes. Of the factors studied herein (T, RH, VP), the amount of water vapor in the air (VP) appears to most clearly control the cracking-climate signal, independent of stress-loading. VP is not commonly considered in mechanical weathering or surface processes studies but is central to theories of crack-tip processes for subcritical cracking in rock and other solids.

Although a precise quantification of long-term climate effects on weathering is beyond the scope of this study, our results suggest Earth climate change on the order of what is predicted for the next 100 years could significantly increase mechanical weathering rates. Therefore, we conclude that past global warming and cooling—like that associated with glacial/interglacial cycles—almost certainly resulted in significant changes in mechanical weathering attributable to the types of climate-driven crack-tip processes supported herein. Thus, our results could provide a new mechanistic explanation for increased sediment production during glacial periods in regions that did not experience freezing temperatures but were wetter (e.g., the desert southwestern United States, as proposed by Persico et al., 2019), or for the extreme variance in global erosion and soil production rates plotted as a function of climate (Perron, 2017; Portenga & Bierman, 2011). Accelerated mechanical weathering under warm wet climates also provides an additional explanatory mechanism for observed strong associations between low-latitude mountain building and global ice ages (Macdonald et al., 2019), or between Earth cooling and land surface reactivity (Rugenstein et al., 2019), or for unexpectedly high erosion rates found in low relief, wet mountainous regions (Adams et al., 2020). Our findings provide a new avenue of exploration for global warming mitigation by weathering (L. L. Taylor et al., 2016) or for understanding the climate-dependent architecture of the critical zone (e.g., West et al., 2014). Perhaps most importantly, they suggest an additional, previously unconsidered mechanism for climate to modulate global weathering rates and thus to stabilize itself, providing a synergy with known pathways involving *chemical* weathering (e.g., Caves et al., 2016; Walker et al., 1981). The next generation of field data, modeling, climate-weathering parameterizations, and rock testing—examined in the framework of climate-dependent subcritical cracking—will enable us to fully integrate this newly identified characteristic of mechanical weathering into the lexicon of global change.

Data Availability Statement

Data presented are available at figshare.com by searching: 10.6084/m9.figshare.12410210.

Acknowledgments

The authors have no identified financial conflict of interest with the results of this paper. This material is based upon work supported by the National Science Foundation under Grant Nos. EAR#0844335, #844401, and #0705277, the University of North Carolina at Charlotte, the Chama Institute of Arts and Sciences, and the Redlair Observatory. Max Dahlquist provided thermal diffusivity measurements and Luke Griffiths porosity measurements for our samples. The following people provided instrumentation, deployment and/or QA/QC assistance: Suraj Swami, Evan Hinson, Jacob Garbini, Luke Browder, Vamsi Krishnaalla, Damika Jones, Gopinath Sundarem, Anup Suggula, Jake Armour, Lawson Armour, Peyton Warren, Oakley Armour, Jaako Putkonen, and Haywood Rankin. Kevin McGoff helped to clarify statistical language in the manuscript. Richard Gangloff, Phil Meredith, Bernard Hallet, Kerry Leith, Peter Mackenzie, Mike Heap, Lyman Persico, Les McFadden, Ellen Wohl, and Jill Marshall provided supportive discussions.

References

Adams, B., Whipple, K., Forte, A., Heimsath, A., & Hodges, K. (2020). Climate controls on erosion in tectonically active landscapes. *Science Advances*, *6*(42), eaaz3166.

Anderson, T. L. (2005). *Fracture mechanics: Fundamentals and applications*, Boca Raton, FL: CRC Press.

Atkinson, B. K. (1987). *Fracture mechanics of rock*. London, England: Academic Press.

Atkinson, B. K., & Meredith, P. G. (1981). Stress corrosion cracking of quartz: A note on the influence of chemical environment. *Tectonophysics*, *77*(1), T1–T11.

Brantut, N., Heap, M., Meredith, P., & Baud, P. (2013). Time-dependent cracking and brittle creep in crustal rocks: A review. *Journal of Structural Geology*, *52*, 17–43.

Burls, N. J., & Fedorov, A. V. (2017). Wetter subtropics in a warmer world: Contrasting past and future hydrological cycles. *Proceedings of the National Academy of Sciences*, *114*(49), 12888–12893.

Byrne, M. P., & O'Gorman, P. A. (2016). Understanding decreases in land relative humidity with global warming: Conceptual model and GCM simulations. *Journal of Climate*, *29*(24), 9045–9061.

Caves, J. K., Jost, A. B., Lau, K. V., & Maher, K. (2016). Cenozoic carbon cycle imbalances and a variable weathering feedback. *Earth and Planetary Science Letters*, *450*, 152–163.

Chadwick, R., Good, P., & Willett, K. (2016). A simple moisture advection model of specific humidity change over land in response to SST warming. *Journal of Climate*, *29*(21), 7613–7632.

Chen, X., Eichhubl, P., Olson, J. E., & Dewers, T. A. (2019). Effect of water on fracture mechanical properties of shales. *Journal of Geophysical Research: Solid Earth*, *124*(3), 2428–2444. https://doi.org/10.1029/2018JB016479

Ching, S. S. (2018). *Acoustic emission and environmental monitoring of two natural granite boulders: Semi-arid vs. temperate environment*, Charlotte, NC: The University of North Carolina at Charlotte.

Collins, B. D., Stock, G. M., Eppes, M. C., Lewis, S., Corbett, S., & Smith, J. (2018). Thermal influences on spontaneous rock dome exfoliation. *Nature Communications*, *9*(1), 1–12.

Daoud, A., Browning, J., Meredith, P. G., & Mitchell, T. M. (2020). Microstructural controls on thermal crack damage and the presence of a temperature-memory effect during cyclic thermal stressing of rocks. *Geophysical Research Letters*, *47*(19), https://doi.org/10.1029/2020GL088693

Dash, L. (2015). *Temperature, strain and acoustic emission monitoring of a natural boulder exposed to the sun* (M.S. Thesis): University of North Carolina at Charlotte.

Dove, P. M. (1995). Geochemical controls on the kinetics of quartz fracture at subcritical tensile stresses. *Journal of Geophysical Research*, *100*(B11), 22349–22359.

Draebing, D., & Krautblatter, M. (2019). The efficacy of frost weathering processes in alpine rockwalls. *Geophysical Research Letters*, *46*(12), 6516–6524. https://doi.org/10.1029/2019GL081981

Draebing, D., Krautblatter, M., & Hoffmann, T. (2017). Thermo-cryogenic controls of fracture kinematics in permafrost rockwalls. *Geophysical Research Letters*, *44*(8), 3535–3544. https://doi.org/10.1002/2016GL072050

Enzel, Y., Amit, R., Grodek, T., Ayalon, A., Lekach, J., Porat, N., et al. (2012). Late Quaternary weathering, erosion, and deposition in Nahal Yael, Israel: An "impact of climatic change on an arid watershed"? *Bulletin*, *124*(5–6), 705–722.

Eppes, M. C., Hancock, G., Chen, X., Arey, J., Dewers, T., Huettenmoser, J., et al. (2018). Rates of subcritical cracking and long-term rock erosion. *Geology*, *46*(11), 951–954.

Eppes, M. C., & Keanini, R. (2017). Mechanical weathering and rock erosion by climate-dependent subcritical cracking. *Reviews of Geophysics*, *55*(2), 470–508. https://doi.org/10.1002/2017RG000557

Eppes, M. C., Magi, B., Hallet, B., Delmelle, E., Mackenzie-Helnwein, P., et al. (2016). Deciphering the role of solar-induced thermal stresses in rock weathering. *Geological Society of America Bulletin*, *128*(9–10), 1315–1338.

Ferrier, K. L., & West, N. (2017). Responses of chemical erosion rates to transient perturbations in physical erosion rates, and implications for relationships between chemical and physical erosion rates in regolith-mantled hillslopes. *Earth and Planetary Science Letters*, *474*, 447–456.

Fletcher, R. C., Buss, H., & Brantley, S. L. (2006). A spheroidal weathering model coupling porewater chemistry to soil thicknesses during steady-state denudation. *Earth and Planetary Science Letters*, *244*(1–2), 444–457.

Gangloff, R. P., & Harlow, D. G. (2017). Interdisciplinary multi-scale research on environment assisted cracking: The 50 year legacy of Robert P. Wei. *International Journal of Fatigue*, *104*(81–98).

Girard, L., Gruber, S., Weber, S., & Beutel, J. (2013). Environmental controls of frost cracking revealed through in situ acoustic emission measurements in steep bedrock. *Geophysical Research Letters*, *40*(9), 1748–1753. https://doi.org/10.1002/grl.50384

Grosse, C. U., & Ohtsu, M. (2008). *Acoustic emission testing*, Heidelberg, Germany: Springer.

Hall, K. (1999). The role of thermal stress fatigue in the breakdown of rock in cold regions. *Geomorphology*, *31*(1), 47–63.

Hall, K., & André, M.-F. (2001). New insights into rock weathering from high-frequency rock temperature data: An Antarctic study of weathering by thermal stress. *Geomorphology*, *41*(1), 23–35.

Hallet, B., Walder, J., & Stubbs, C. (1991). Weathering by segregation ice growth in microcracks at sustained subzero temperatures: Verification from an experimental study using acoustic emissions. *Permafrost and Periglacial Processes*, *2*(4), 283–300.

Heap, M. J., Baud P., Meredith P. G. (2009). Influence of temperature on brittle creep in sandstones. *Geophysical Research Letters*, *36*(19), https://doi.org/10.1029/2009gl039373

Hilley, G., Chamberlain, C., Moon, S., Porder, S., & Willett, S. (2010). Competition between erosion and reaction kinetics in controlling silicate-weathering rates. *Earth and Planetary Science Letters*, *293*(1–2), 191–199.

Holbrook, W. S., Marcon, V., Bacon, A. R., Brantley, S. L., Carr, B. J., Flinchum, B. A., et al. (2019). Links between physical and chemical weathering inferred from a 65-m-deep borehole through Earth's critical zone. *Scientific Reports*, *9*(1), 4495.

Isson, T., Planavsky, N., Coogan, L., Stewart, E., Ague, J., Bolton, E., et al. (2020). Evolution of the global carbon cycle and climate regulation on earth. *Global Biogeochemical Cycles*, *34*(2), e2018GB006061.

Kasting, J. F. (2019). The Goldilocks planet? How silicate weathering maintains earth "just right". *Elements: An International Magazine of Mineralogy, Geochemistry, and Petrology*, *15*(4), 235–240.

Lu, M., & Hedin, L. O. (2019). Global plant–symbiont organization and emergence of biogeochemical cycles resolved by evolution-based trait modelling. *Nature Ecology & Evolution*, *3*(2), 239–250.

Lobo-Guerrero, S., & Vallejo, L. E. (2006). Application of Weibull statistics to the tensile strength of rock aggregates. *Journal of geotechnical and geoenvironmental engineering*, *132*(6), 786–790.

Macdonald, F. A., Swanson-Hysell, N. L., Park, Y., Lisiecki, L., & Jagoutz, O. (2019). Arc-continent collisions in the tropics set Earth's climate state. *Science*, *364*(6436), 181–184.

Marshall, J. A., Roering, J. J., Gavin, D. G., & Granger, D. E. (2017). Late Quaternary climatic controls on erosion rates and geomorphic processes in western Oregon, USA. *GSA Bulletin*, *129*(5–6), 715–731.

Martel Stephen J. (2011). Mechanics of curved surfaces, with application to surface-parallel cracks. *Geophysical Research Letters*, *38*(20), http://dx.doi.org/10.1029/2011gl049354

Matsukura, Y., & Takahashi, K. I. (2000). A new technique for rapid and non-destructive measurement of rock-surface moisture content; preliminary application to weathering studies of sandstone blocks. *Developments in Geotechnical Engineering*, *84*, 47–54.

Matsuoka, N. (1990). The rate of bedrock weathering by frost action: Field measurements and a predictive model. *Earth Surface Processes and Landforms*, *15*(1), 73–90.

Meredith, P., & Atkinson, B. (1985). Fracture toughness and subcritical crack growth during high-temperature tensile deformation of Westerly granite and Black gabbro. *Physics of the earth and planetary interiors*, *39*(1), 33–51.

Molaro, J., & Byrne, S. (2015). Grain-Scale thermoelastic stresses and spatiotemporal temperature gradients on airless bodies, implications for rock breakdown. *Journal of Geophysical Research: Planets*, *120*(2), 255–277. https://doi.org/10.1002/2014JE004729

Molnar Peter (2004). Interactions among topographically induced elastic stress, static fatigue, and valley incision. *Journal of Geophysical Research: Earth Surface*, *109*(F2), http://dx.doi.org/10.1029/2003jf000097

Moon, S., Perron, J. T., Martel, S. J., Goodfellow, B. W., Ivars, D. M., Simeonov, A., et al. (2019). *Landscape features influence bedrock fracture openness in the deep subsurface*. Proceedings GSA Annual Meeting in Phoenix, Arizona, USA.

Moon, S., Perron J. T., Martel S. J., Goodfellow B. W., Mas Ivars D., Hall A., et al. (2020). Present-day stress field influences bedrock fracture openness deep into the subsurface. *Geophysical Research Letters*, *47*(23), http://dx.doi.org/10.1029/2020gl090581

Murphy, B. P., Johnson, J. P., Gasparini, N. M., & Sklar, L. S. (2016). Chemical weathering as a mechanism for the climatic control of bedrock river incision. *Nature*, *532*(7598), 223–237.

Murton, J. B., Peterson, R., & Ozouf, J.-C. (2006). Bedrock fracture by ice segregation in cold regions. *Science*, *314*(5802). 1127–1129.

Nara, Y., Hiroyoshi, N., Yoneda, T., & Kaneko, K. (2010). Effects of relative humidity and temperature on subcritical crack growth in igneous rock. *International Journal of Rock Mechanics and Mining Sciences*, *47*(4), 640–646.

Nara, Y., Kashiwaya, K., Nishida, Y., & Ii, T. (2017). Influence of surrounding environment on subcritical crack growth in marble. *Tectonophysics*, *706–707*, 116–128.

Pederson, J., Pazzaglia, F., & Smith, G. (2000). Ancient hillslope deposits: Missing links in the study of climate controls on sedimentation. *Geology*, *28*(1), 27–30.

Peng Sheng, Hu Qinhong, Hamamoto Shoichiro (2012). Diffusivity of rocks: Gas diffusion measurements and correlation to porosity and pore size distribution. *Water Resources Research*, *48*(2), http://dx.doi.org/10.1029/2011wr011098

Perron, J. T. (2017). Climate and the pace of erosional landscape evolution. *Annual Review of Earth and Planetary Sciences*, *45*, 561–591.

Persico, L., McFadden, L., & McAuliffe, J. (2019). *Climatic controls on the timing of hillslope soil formation and erosion in the eastern Mojave Desert* (Vol. 51, No. 5). Geological Society of America Abstracts with Programs.

Phillipson, M. C., Emmanuel, R., & Baker, P. H. (2016). The durability of building materials under a changing climate. *Wiley Interdisciplinary Reviews: Climate Change*, *7*(4), 590–599.

Portenga, E. W., & Bierman, P. R. (2011). Understanding Earth's eroding surface with 10 Be. *Geological Society of America Today*, *21*(8), 4–10.

Ravaji Babak, Alí-Lagoa Víctor, Delbo Marco, Wilkerson Justin W. (2019). Unraveling the Mechanics of Thermal Stress Weathering: Rate-Effects, Size-Effects, and Scaling Laws. *Journal of Geophysical Research: Planets*, *124*(12), 3304–3328. http://dx.doi.org/10.1029/2019je006019

Rempel, A. W., Marshall, J. A., & Roering, J. J. (2016). Modeling relative frost weathering rates at geomorphic scales. *Earth and Planetary Science Letters*, *453*, 87–95.

Richter, D. D., Eppes, M. C., Austin, J. C., Bacon, A. R., Billings, S. A., Brecheisen, Z., et al. (2019). Soil production and the soil geomorphology legacy of Grove Karl Gilbert. *Soil Science Society of America Journal*, *84*(1), 1–20.

Rugenstein, J. K. C., Ibarra, D. E., & von Blanckenburg, F. (2019). Neogene cooling driven by land surface reactivity rather than increased weathering fluxes. *Nature*, *571*(7763), 99–102.

Scheff, J., Seager, R., Liu, H., & Coats, S. (2017). Are glacials dry? Consequences for paleoclimatology and for greenhouse warming. *Journal of Climate*, *30*(17), 6593–6609.

Scott, D. N., & Wohl, E. E. (2019). Bedrock fracture influences on geomorphic process and form across process domains and scales. *Earth Surface Processes and Landforms*, *44*(1), 27–45.

Sklar, L. S., Riebe, C. S., Marshall, J. A., Genetti, J., Leclere, S., Lukens, C. L., & Merces, V. (2017). The problem of predicting the size distribution of sediment supplied by hillslopes to rivers. *Geomorphology*, *277*, 31–49.

Stock, G. M., Martel, S. J., Collins, B. D., & Harp, E. L. (2012). Progressive failure of sheeted rock slopes: The 2009–2010 Rhombus Wall rock falls in Yosemite Valley, California, USA. *Earth Surface Processes and Landforms*, *37*(5), 546–561.

Taylor, L. L., Quirk, J., Thorley, R. M., Kharecha, P. A., Hansen, J., Ridgwell, A., et al. (2016). Enhanced weathering strategies for stabilizing climate and averting ocean acidification. *Nature Climate Change*, *6*(4), 402–406.

Taylor, K. E., Stouffer, R. J., & Meehl, G. A. (2012). An overview of CMIP5 and the experiment design. *Bulletin of the American Meteorological Society*, *93*(4), 485–498.

Tsonis, A. A. (2002). *An introduction to atmospheric thermodynamics*, Cambridge, UK: Cambridge University Press.

Viles, H. A. (2005). Microclimate and weathering in the central Namib Desert, Namibia. *Geomorphology*, *67*(1), 189–209.

Viles, H. A. (2013). Synergistic weathering processes In Treatise on geomorphology (Vol. 4).

Voigtländer, A., Leith, K., & Krautblatter, M. (2018). Subcritical crack growth and progressive failure in Carrara marble under wet and dry conditions. *Journal of Geophysical Research: Solid Earth*, *123*(5), 3780–3798. https://doi.org/10.1029/2017JB014956

Walder, J., & Hallet, B. (1985). A theoretical model of the fracture of rock during freezing. *Geological Society of America Bulletin*, *96*(3), 336–346.

Walker, J. C., Hays, P., & Kasting, J. F. (1981). A negative feedback mechanism for the long-term stabilization of Earth's surface temperature. *Journal of Geophysical Research*, *86*(C10), 9776–9782.

Warren, K., Eppes, M.-C., Swami, S., Garbini, J., & Putkonen, J. (2013). Automated field detection of rock fracturing, microclimate, and diurnal rock temperature and strain fields. *Geoscientific Instrumentation, Methods and Data Systems Discussions*, *3*(2), 371–406.

West, N., Kirby, E., Bierman, P., & Clarke, B. A. (2014). Aspect-dependent variations in regolith creep revealed by meteoric 10Be. *Geology*, *42*(6), 507–510.

Winnick, M. J., & Maher, K. (2018). Relationships between CO_2, thermodynamic limits on silicate weathering, and the strength of the silicate weathering feedback. *Earth and Planetary Science Letters*, *485*, 111–120.